Originally published as:

RMetS

Royal Meteorological Society

Assessing 20th century climate–vegetation feedbacks of land-use change and natural vegetation dynamics in a fully coupled vegetation–climate model

Bart J. Strengers,[a]* Christoph Müller,[a,b] Michiel Schaeffer,[c,d] Reindert J. Haarsma,[e]
Camiel Severijns,[e] Dieter Gerten,[b] Sibyll Schaphoff,[b] Roy van den Houdt[a]
and Rineke Oostenrijk[a]

[a] *Netherlands Environmental Assessment Agency (PBL), Postbus 303, 3720 AH Bilthoven, The Netherlands*
[b] *Potsdam Institute for Climate Impact Research (PIK), PO Box 60 12 03, 14412 Potsdam, Germany*
[c] *Climate Analytics GmbH c/o Potsdam Institute for Climate Impact Research (PIK), PO Box 60 12 03, 14412 Potsdam, Germany*
[d] *Environmental Systems Analysis Group, Wageningen University & Research Centre (WUR), PO Box 47, 6700 AA Wageningen, The Netherlands*
[e] *Royal Netherlands Meteorological Institute (KNMI), Postbus 201, 3730 AE De Bilt, The Netherlands*

ABSTRACT: This study describes the coupling of the dynamic global vegetation model (DGVM), Lund–Potsdam–Jena Model for managed land (LPJmL), with the general circulation model (GCM), Simplified Parameterizations primitivE Equation DYnamics model (SPEEDY), to study the feedbacks between land-use change and natural vegetation dynamics and climate during the 20th century. We show that anthropogenic land-use change had a stronger effect on climate than the natural vegetation's response to climate change (e.g. boreal greening). Changes in surface albedo are an important driver of the climate's response; but, especially in the (sub)tropics, changes in evapotranspiration and the corresponding changes in latent heat flux and cloud formation can be of equal importance in the opposite direction. Our study emphasizes that implementing dynamic vegetation into climate models is essential, especially at regional scales: the dynamic response of natural vegetation significantly alters the climate change that is driven by increased atmospheric greenhouse gas concentrations and anthropogenic land-use change. Copyright © 2010 Royal Meteorological Society

Additional Supporting information may be found in the online version of this article.

1. Introduction

Climate and vegetation strongly interact at local to global scales: while the climate exerts a dominant control on the spatial distribution of the major vegetation types at the global scale, vegetation cover affects climate via its physical characteristics (biogeophysical mechanisms) and via gas exchange with the atmosphere (biogeochemical effects) (Brovkin *et al.*, 2006).

Land-use and land-cover change (LULCC) have been the most important drivers of changes in vegetation patterns and, thus, in land surface properties in the past, and they yield high potential to do so in the future (Strengers *et al.*, 2004; Schaeffer *et al.*, 2006; Müller *et al.*, 2007). Changes in vegetation composition can have significant effects on climate due to many positive and negative feedbacks, not only at the regional scale but also at the global scale.

Figure 1 is an illustration of the main aspects of the *local* feedbacks involved for a globally important type of LULCC: large-scale deforestation for agriculture. Principally, deforestation increases the surface albedo (Myhre and Myhre, 2003) and decreases evapotranspiration because grasses and annual crops cannot access as much soil water as trees can for transpiration. The increase in albedo decreases surface short-wave radiation (SSR) and therefore surface temperatures (blue in Figure 1). Lower surface temperatures cause an additional reduction in evapotranspiration, causing less latent cooling, leaving more sensible heat to warm the surface again, and thus forming a negative feedback loop (green in Figure 1). In temperate and boreal regions, the albedo-driven cooling is often considered to be the dominant factor (Govindasamy *et al.*, 2001; Bounoua *et al.*, 2002; Matthews *et al.*, 2004; Brovkin *et al.*, 2006; Bala *et al.*, 2007).

Especially in the (sub)tropics reduced evapotranspiration is more important, also because it reduces convective cloud formation and thus convective precipitation. This again lowers evapotranspiration, forming a

---

* Correspondence to: Bart J. Strengers, Netherlands Environmental Assessment Agency (PBL), Postbus 303, 3720 AH Bilthoven, The Netherlands. E-mail: bart.strengers@pbl.nl

Figure 1. Conceptual causal loop diagram of the effects of deforestation on the local climate system; '−' indicates negative interaction (if higher a, then lower b *or* if lower a, then higher b); '+' indicate positive interactions (if higher a, then higher b *or* if lower a, then lower b). SSR is surface short-wave downward radiation, PBL is planetary boundary layer, and *T* is temperature. Colours indicate the different pathways involved; for details, see text. This figure is available in colour online at wileyonlinelibrary.com/journal/joc

positive feedback loop (black in Figure 1). Furthermore, decreasing cloud cover decreases albedo, and therefore the initial increase in surface albedo is also counter-balanced by reduced cloud formation. Many studies show that these counter-balancing factors result, in the end, in limited tropical cooling compared to the extra-tropics (Brovkin *et al.*, 2006) or even in a warming (Bounoua *et al.*, 2002; Bala *et al.*, 2007).

Deforestation also reduces the roughness length for momentum and thus the turbulence in the planetary boundary layer (PBL). Reduced turbulence in the PBL directly reduces the sensible heat flux, a mechanism that is counter-balanced by an indirect increase through reduced evapotranspiration (red in Figure 1). In principle, the overall contribution of changes in roughness length to surface temperature changes is relatively small compared to other factors, although the contribution to changes in evapotranspiration can be substantial (Costa and Foley, 2000; Matthews *et al.*, 2003; Oyama and Nobre, 2004).

Finally, there is a relatively strong biogeochemical impact that raises temperatures through radiative forcing of higher atmospheric CO_2 concentrations (purple in Figure 1), and plants can also obtain CO_2 more efficiently from the atmosphere and can, on average, close their stomata more often, which reduces evapotranspiration (yellow in Figure 1) (Cox *et al.*, 2004; Friedlingstein *et al.*, 2006; O'Ishi *et al.*, 2009).

Remote effects that can result from LULCC and changes in natural vegetation, such as remote changes in rainfall through planetary wave propagation (Gedney and Valdes, 2000), changes in Hadley cell and Walker cell circulations due to LULCC in the Tropics and south-east Asia (Chase *et al.*, 2000; Zhao and Pitman, 2002), or other teleconnections such as those associated with El Niño-Southern Oscillation (ENSO) events due to

deforestation of the Asian tropical region, are not shown in Figure 1 (Mabuchi *et al.*, 2005). There are several studies claiming that remote effects are not relevant or at least are highly uncertain (Findell *et al.*, 2007; Pitman *et al.*, 2009). Principally, there is consensus that vegetation patterns and LULCC significantly affect regional climate, while there is still debate about the role of vegetation and LULCC impacts on global scale climate (Pitman *et al.*, 2009).

Many studies on climate–vegetation interaction use general circulation models (GCMs) coupled with the so-called land surface schemes (LSSs), which cover the interactions on short timescales (i.e. seconds to hours), dominated by the rapid biophysical and biogeochemical processes that exchange energy, water, carbon dioxide, and momentum between atmosphere and land surface. These types of studies use prescribed vegetation patterns, and focus either on one or more regions where strong climate–vegetation interactions are expected such as the Amazon (Gedney and Valdes, 2000; Voldoire and Royer, 2004; Avissar and Werth, 2005; Dickinson *et al.*, 2006), northern Africa (Claussen, 1997; Voldoire and Royer, 2004; Maynard and Royer, 2004a, 2004b), or the northern high latitudes (Brovkin *et al.*, 2003; Levis and Bonan, 2004; Jahn *et al.*, 2005). Other studies were conducted for the global level (Kleidon *et al.*, 2000; Koster *et al.*, 2006; Bala *et al.*, 2007), sometimes taking into account patterns of anthropogenic LULCC (Chase *et al.*, 2000; Betts, 2001; Bounoua *et al.*, 2002; Feddema *et al.*, 2005; Brovkin *et al.*, 2006; Pitman *et al.*, 2009).

A second important class of climate–vegetation studies also takes into account the intermediate-timescale (i.e. days to months) processes such as changes in soil moisture, carbon allocation, and vegetation phenology

(e.g. budburst, leaf-out, senescence, dormancy), and processes on even longer timescales (i.e. seasons, years, and decades), related to changes in the vegetation structure itself by coupling a dynamic global vegetation model (DGVM) with the climate model used. Foley *et al*. (1998) were among the first who noted the importance of explicitly modelling dynamic vegetation in climate models. Many studies included vegetation dynamics in either regional studies, e.g. the Amazon (Cox *et al*., 2000, 2004; Cowling *et al*., 2008), North Africa (Doherty *et al*., 2000; Notaro and Liu, 2008) or the northern high latitudes (Notaro and Liu, 2007; Cook *et al*., 2008), or at the global scale (Delire *et al*., 2004; Gallimore *et al*., 2005; Notaro *et al*., 2005; Bonan and Levis, 2006; Friedlingstein *et al*., 2006; Notaro and Liu, 2007). However, there are hardly any studies that take into account effects of both LULCC *and* dynamic natural vegetation on the climate in a single modelling framework. Analysing both effects simultaneously in a consistent framework is important because direct human LULCC (e.g. deforestation) may act in the same (e.g. spreading of deserts due to reduced precipitation) or opposite direction of natural vegetation dynamics (e.g. boreal greening). Also, areas of LULCC and natural vegetation's response to climate change partially overlap and therefore natural vegetation's response is at least partially overruled by anthropogenic LULCC. A study that *does* analyse both aspects is provided by Matthews *et al*. (2004), who showed that the biogeophysical cooling, mainly Northern Hemispheric, due to LULCC (or a reduction in the warming if all natural and anthropogenic forcings are considered) since 1700 is amplified by a positive feedback between vegetation dynamics and the climate system.

During the 20th century, there has been a strong increase in anthropogenic greenhouse gas (GHG) emissions, resulting in climate shifts at global and regional scales. In the same period, significant LULCC have also occurred. How these LULCC have modified and possibly counteracted the climate shifts due to an increase in anthropogenic GHGs is not well understood. In this study, we have investigated, at the global scale, the relative roles of natural vegetation dynamics and LULCC in the biogeophysical interaction between climate and vegetation during the 20th century. For this, the GCM Simplified Parameterizations primitivE Equation DYnamics model (SPEEDY) (Molteni, 2003) was coupled with the DGVM Lund–Potsdam–Jena Model for managed land (LPJmL) (Sitch *et al*., 2003; Gerten *et al*., 2004; Bondeau *et al*., 2007) on a 40-min time-step basis. As indicated above, increasing atmospheric CO_2 concentrations also affect plant productivity and stomatal conductance, and thus evapotranspiration (yellow in Figure 1). Even though these effects are explicitly accounted for in all our experiments, as LPJmL employs the Farquhar photosynthesis model (Farquhar *et al*., 1980), as modified by Collatz *et al*. (1991, 1992), we do not explicitly analyse the effects of CO_2 fertilization on stomatal conductance in this study.

2. Methodology

2.1. The SPEEDY model

SPEEDY has been developed at the International Centre for Theoretical Physics (ICTP) in Trieste (Italy) and has been described in full detail by Molteni (2003). The model has eight layers in the vertical and a spectral truncation at total wave number 30 (T30), corresponding to a spatial resolution of 3.75° latitude and longitude. The model contains parameterization schemes for large-scale condensation, convection, clouds, radiative fluxes, surface fluxes, and vertical diffusion, and is based on the same physical principles adopted in the schemes of state-of-the-art atmosphere GCMs (AGCMs). The basic time step is 40 min. A limitation of the current version of SPEEDY is the omission of aerosols. Computationally, SPEEDY is 1 order of magnitude faster than a state-of-the-art AGCM at the same horizontal resolution, whereas the quality of the simulated climate and patterns of variability in the free atmosphere compare well with these models and with observations (Hazeleger *et al*., 2003; Molteni, 2003). Various studies with SPEEDY have demonstrated its ability to simulate the dominant responses to surface anomalies (Haarsma *et al*., 2003; Bracco *et al*., 2007; Haarsma and Hazeleger, 2007; Kucharski *et al*., 2007, 2008; Sterl *et al*., 2007; Kucharski *et al*., 2009). It is therefore suitable for studies on climate–vegetation feedbacks and inter-decadal or inter-centennial variability. The original SPEEDY model was coupled to a simple land bucket model (LBM), as described by Haarsma *et al*. (1998). Besides the limitations of such a simple representation of the land's surface, the main deficiency of this coupled system was the daily data exchange between the models. Such a time step is not sufficient to simulate the highly nonlinear process of boundary layer build-up and related energy fluxes during daytime.

For our experiments and the coupling to LPJmL, we extended SPEEDY by a diurnal cycle (instead of an everlasting half-light), a dynamic boundary layer over land, based on Ronda *et al*. (2003), and an exchange of data with LPJmL at every 40-min time step (see Section 2.3). A detailed description of the extentions made to SPEEDY can be found in the Supporting Information 1.

2.2. The DGVM LPJmL

The LPJmL is described in detail by Sitch *et al*. (2003), Gerten *et al*. (2004), Bondeau *et al*. (2007). LPJmL employs nine plant functional types (PFTs, derived from traits based on species morphology, physiology, and/or life history) to simulate natural vegetation, of which seven are woody (two tropical, three temperate, two boreal) and two herbaceous. In addition to the attributes controlling physiology and dynamics, each PFT is assigned bioclimatic limits, which determine whether it can survive or regenerate under the climatic conditions prevailing in a particular grid cell at a particular point in time. Unlike previous models in the BIOME family, LPJmL also includes explicit representations

of vegetation structure, dynamics, competition between PFTs, and soil biogeochemistry. Agricultural land is implemented via 11 crop functional types (CFTs) as described by Bondeau *et al.* (2007). Each grid cell is simulated as a mosaic divided into fractional coverage of PFTs, agricultural land with single CFT stands, and bare ground. This concept provides a simple method for scaling-up processes acting at the level of an individual plant to the vegetation stand over a grid cell instead of aggregation of properties to those of generalized biomes. This consideration of sub-grid landscape variability is important for accurately determining surface fluxes that are essential for coupling to climate models.

Survival and establishment of PFTs is based on their energy and carbon balance (net primary production, NPP), as well as a few bioclimatic limits, which are based on 20-year running means. Each PFT population is characterized by a set of variables describing the state of the average individual, and by the population density. Fire, the most important natural disturbance at the global scale, is explicitly represented in LPJmL.

We applied the following changes to the original LPJmL for coupling with SPEEDY:

- The daily time step of energy and water exchange with the atmosphere (interception, canopy conductance, potential evapotranspiration) was decreased to a sub-daily time step (i.e. 40 min), which has implications for the simulation of plant performance.
- The simple soil temperature scheme, which followed prescribed air temperatures with a temporal lag (Sitch *et al.*, 2003), was replaced by introducing a five-layer soil and snow scheme, based on van den Hurk *et al.* (2000) for the two snow layers and on EC-Bilt (Opsteegh *et al.*, 1998) for the three soil layers.
- The freezing and melting processes of soil moisture were included.
- Grid cells covered by ice were introduced, as climate modelling is not limited to vegetated areas only.
- Vegetation roughness was computed as described in the Supporting Information 1.7, which affected the turbulence in the boundary layer.
- Albedo was computed depending on land surface conditions and based on a combination of assumed albedo values for bare soil, trees (leaf bearing *vs* leafless), snow (snow on bare soil *vs* snow on leaves), litter, grass, and crops (see Supporting Information 1.8).

The most fundamental change was the switch to a sub-daily time step (Supporting Information 2), which also caused an increase in the computation time by a factor of 15. The sub-daily version of LPJmL resembles results of the daily original version, but displays some minor differences in vegetation composition and performance. For more details, see Supporting Information 2.

Carbon assimilation is also affected by enzymatic reactions that do not respond in 40-min intervals. Therefore, carbon assimilation is still computed at daily time steps, based on the sub-daily canopy conductance and

energy flow in all 36 time intervals of one simulation day. Matching the spatial resolution of SPEEDY, LPJmL was also run at a spatial resolution of 3.75°. Müller and Lucht (2007) showed that reducing the spatial resolution of LPJmL simulations causes only small deviations from simulations at finer resolutions, which is mainly due to averaging out of climatic extremes, but considerably reduces computation time.

2.3. Coupling the DGVM LPJmL to SPEEDY

In Supporting Information 1, the interaction between LPJmL and SPEEDY is described in detail. More generally, the following information is exchanged from SPEEDY to LPJmL at every time step (40 min):

- The maximum evapotranspiration rate as limited by the difference between the actual relative humidity and saturated air is used to compute the latent heat flux (LHF) in LPJmL.
- A scaling factor for turbulence of the boundary layer used to compute the sensible heat flux (SHF).
- SSR to compute photosynthesis and the heat that enters the soil.
- The downward surface longwave radiation (SLRD), which is the second heat component determining soil temperature.
- The 2-m temperature used in the computation of the SHF, photosynthesis, and, on an yearly basis, establishment and die back of vegetation.
- Precipitation (rain and snow separately).

In turn, LPJmL provides the following data to SPEEDY at every 40-min time step:

- The LHF, composed of evaporation from bare soil, transpiration from vegetation, and interception.
- The SHF.
- The roughness length for momentum used in the computation of the drag coefficient.
- Surface albedo.

In this exploratory study, prescribed sea surface temperatures (SSTs taken from HadISST1.1, ftp://www.iges.org/pub/kinter/c20c/HadISST/) were used. Also, we used prescribed historical atmospheric CO_2 concentrations as we focused on the biogeophysical aspects of the climate–vegetation interaction rather than on carbon-cycle feedbacks.

It should be noted that we did not employ any flux corrections or climate anomalies to simulated vegetation patterns with LPJmL. Therefore, climate distortions (i.e. deviations from the real situation) in SPEEDY directly affected vegetation patterns.

2.4. Experiments

We compare four different simulation experiments that have been conducted with the coupled SPEEDY–LPJmL model. We compare different vegetation settings to study the impact of dynamic vegetation on climate simulations,

covering the historical period from 1871 to 2007. In two experiments, we simulate natural vegetation only ('Na' experiments), excluding the effects of land-use change, focusing on the feedbacks between dynamic vegetation and climate simulations. In two other simulations ('LUC'), we include prescribed patterns of anthropogenic land-use change, which are updated annually based on linear interpolations of the 10-year interval supplied by the HYDE data base (Klein Goldewijk *et al.*, 2007) (see Figure S1, Supporting Information 3). Both the Na and LUC experiments were computed once with static prescribed vegetation patterns ('Fi') and once with dynamic vegetation ('Dy'), in which the composition of natural vegetation was allowed to respond to changes in climate as simulated by SPEEDY.

For each of the four experiments, a small random distortion of the initial skin layer temperature is applied to five individual ensemble members. Averaging over the whole ensemble then improves the ratio of signal (impact of change in deterministic boundary conditions) to noise (stochastic internal climate variability). We present only results that are significant at the 99% confidence level (see Section 3) according to the Student's *t*-test.

To generate suitable starting conditions, SPEEDY has been run coupled with LPJmL for 500 years using stable GHG-concentrations and SSTs of 1870 to bring vegetation patterns into equilibrium with the climate of 1870 as simulated by SPEEDY. This equilibrium vegetation pattern is used as the initial state for the experiments of this study. The spin-up has been run with and without agricultural land-use (i.e. crops and pasture) of 1870 (Klein Goldewijk *et al.*, 2007), which resulted in the initial state for the land-use change experiments (LUC) and experiments with natural vegetation only (Na), respectively. These two starting vegetation patterns allow for better analysis of the effects of LUC and dynamic vegetation, as vegetation is in equilibrium with simulated climate (which is dependent on the vegetation pattern).

All experiments are transient runs from 1871 to 2007, based on these equilibria vegetation patterns and prescribed and observed GHG-concentrations and SSTs.

The differences between the ensemble-average of the Fi and Dy-experiments show the impact of dynamic vegetation patterns on climate and vice versa, with and without LUC. The differences between the Na and LUC experiments show the impact of LUC and/or dynamic vegetation on climate.

3. Results

3.1. Model performance

We compared the forest cover patterns of the coupled SPEEDY–LPJmL models with the International Geosphere-Biosphere Programme (IGBP) DISCover data set (Loveland *et al.*, 2000) by applying the Fuzzy Numerical statistic. This method has been developed by the Research Institute for Knowledge Systems and implemented in the Map Comparison Kit (MCK) as developed
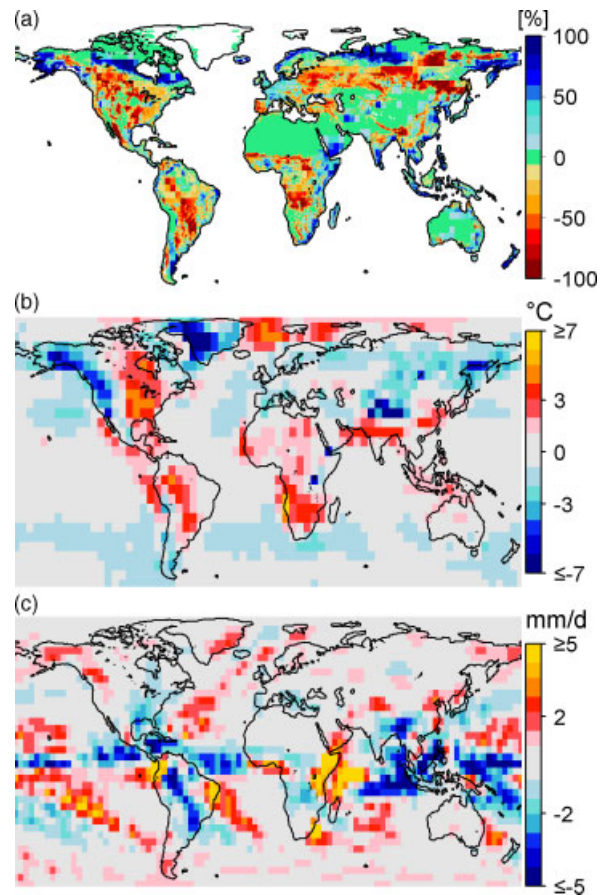

Figure 2. (a) Difference of tree cover as reported by IGBP DISCover 2000 (Loveland *et al.*, 2000) and SPEEDY/LPJmL (experiment DyLUC) in the year 2000. Negative values indicate that simulated forest fractions are lower than DISCover; (b) difference between observed 2-m temperatures from the Climatic Research Unit (CRU) data (Jones *et al.*, 1999) and experiment DyLUC over the period 1961–1990 (DyLUC minus CRU); (c) difference between precipitation from the Climate Prediction Center Merged Analysis of Precipitation (CMAP) data set (Xie and Arkin, 1997) and experiment DyLUC (DyLUC minus CMAP), covering the period 1979–2001. In (b) and (c), the colours red and yellow indicate an overestimation (i.e. too high temperatures *vs* too high precipitation levels) of model results as compared to the data and blue indicates an underestimation. This figure is available in colour online at wileyonlinelibrary.com/journal/joc

by the Netherlands Environmental Assessment Agency. The method follows the rationale of the fuzzy Kappa measure (Hagen, 2003; Hagen-Zanker *et al.*, 2005), is adjusted to work with continuous instead of categorical data, and is documented in the MCK user manual (Hagen-Zanker *et al.*, 2006). It is a very strict comparison measure, as it disregards matches that can be expected by chance. Our comparison (Figure 2(a)) results in a fuzzy numerical Kappa of 0.41, which is considered to be a 'moderate' agreement. For some regions, like northwestern Europe, the United Kingdom, India, and south-east China, natural forests are dense forests and therefore the simulated overestimation of trees in these regions can only be due to an underestimation of tree cover in the data or due to land-use categories in the DISCover data that have not been considered here (e.g. urban area and infrastructure). Other deviations in
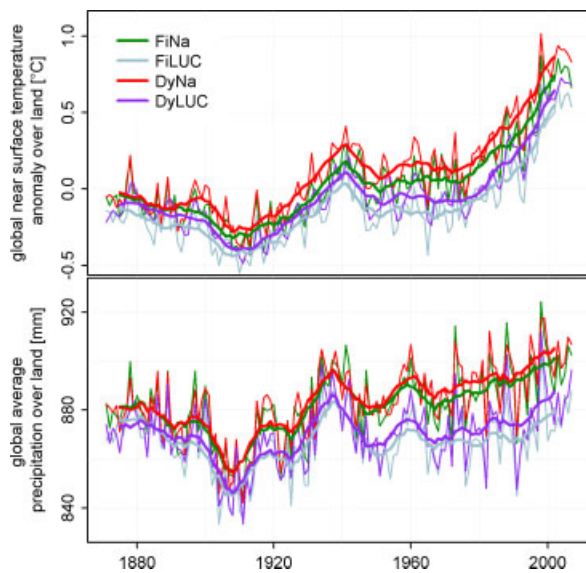
Figure 3. Ensemble-mean global average (a) near-surface tempera-ture change over land as compared to the 1960–1990 average of experiment DyLUC and (b) yearly precipitation over land in the four experiments (excluding Greenland and Antarctica). Bold lines repre-sent 10-year running means. This figure is available in colour online at wileyonlinelibrary.com/journal/joc

especially in the precipitation pattern (Figure 2(c)), are common for many GCMs operating at the same grid size as ours (Solomon *et al.*, 2007; Gleckler *et al.*, 2008). Furthermore, SPEEDY has a warm bias (Figure 2(b)), which is, among others, due to the omission of anthro-pogenic aerosols. In general, tree cover is underestimated in regions where precipitation is too low and temperatures are too high, e.g. in south-west Amazonia, central United States, and the Sahel, while tree cover is overestimated in some semi-arid regions where simulated precipitation is too high, e.g. around the Horn of Africa.

3.2. Global average climate response to LULCC and vegetation dynamics

In our experiments, in the last 20 years of the simula-tion period, anthropogenic LULCC causes global average cooling (or reduced warming) over land without perma-nent ice cover (i.e. the globe excluding the oceans as well as Greenland and Antarctica) of 0.20 °C when natural vegetation is fixed (FiNa *vs* FiLUC, see Figure 3(a)) and 0.22 °C with dynamic vegetation (DyNa *vs* DyLUC), i.e. dynamics of natural vegetation act as a (small) positive feedback.

The main driver of the cooling (or reduced warming) due to LULCC is the increase in albedo and the following decrease in SSR due to deforestation, which, at least at the global level, more than outweighs the decrease in LHF (Figures 4 and 5), and, to a lesser extent, cloud cover (not shown). For the global response over land, the reduced warming due to LULCC is far more important than the

vegetation patterns can be explained by typical vegetation biases of LPJmL, such as the northward tree line bias (Sitch *et al.*, 2003), the lack of a shrub PFT, and the lack of permafrost dynamics, whereas some are due to deviations in simulated climate. The latter deviations,
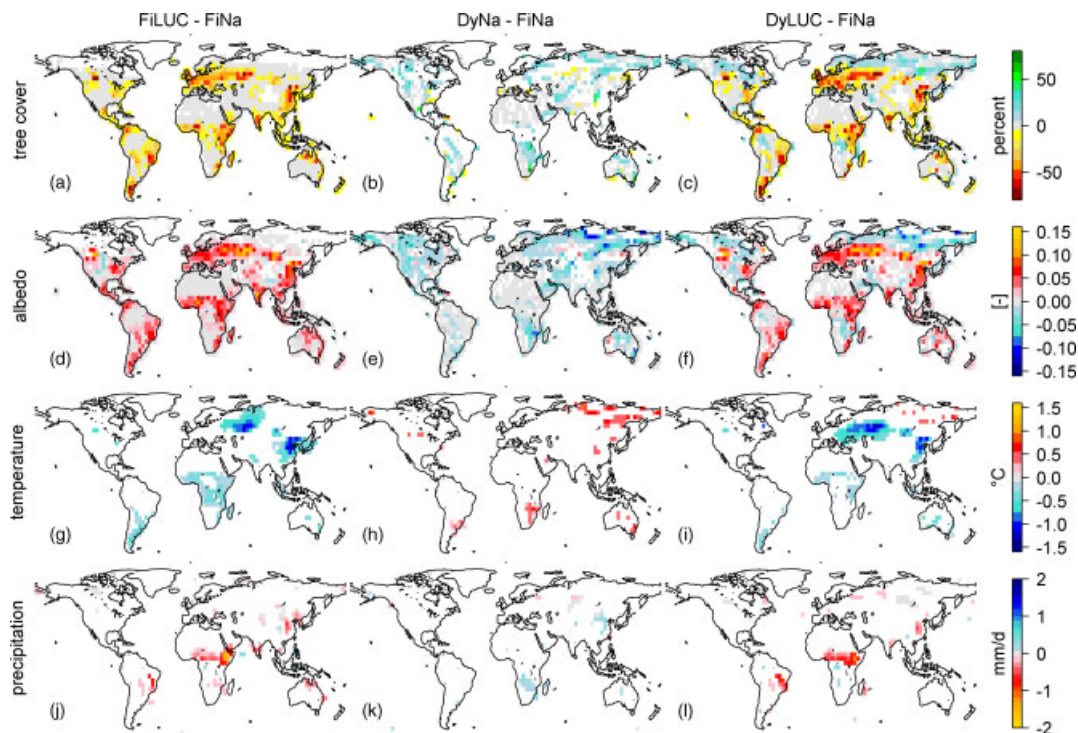
Figure 4. Difference in tree cover fraction, albedo, yearly average near-surface air temperature (K) and precipitation (mm/day) due to land-use change (FiLUC minus FiNa, first column), dynamic vegetation (DyNa minus FiNa, second column), and due to the *combined* effect of both dynamic vegetation *and* LUC (DyLUC minus FiNa, third column), averaged over the period 1988–2007. Only areas where changes are significant at the 99% confidence level are shown. This figure is available in colour online at wileyonlinelibrary.com/journal/joc
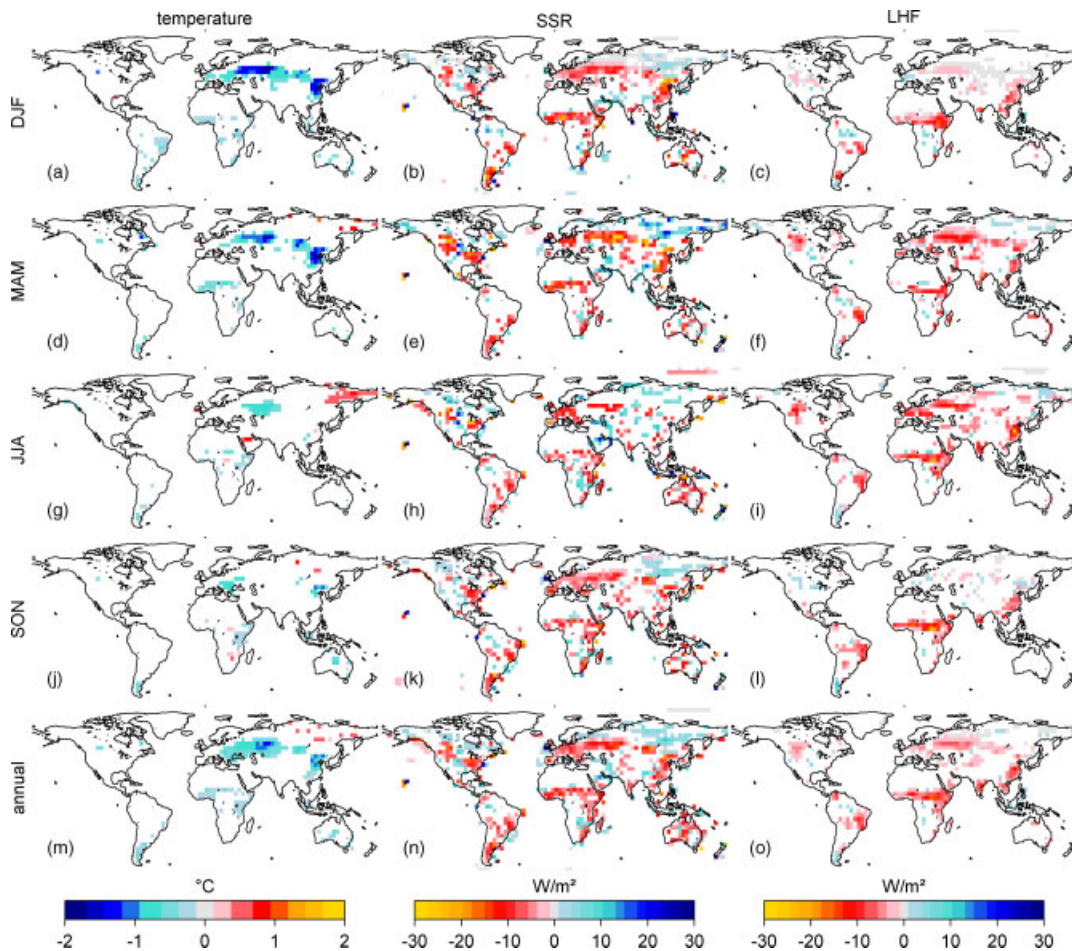
Figure 5. Seasonal and annual differences in temperature (first column), SSR (second column, downward flux), and LHF (third column, upward flux) between the experiments DyLUC and FiNa (DyLUC minus FiNa, i.e. the *combined* effect of both dynamic vegetation *and* LUC), averaged over the period 1988–2007. First row is the mean of December, January, February (DJF), second row is the mean of March, April, May (MAM), third row is the mean of June, July, August (JJA), fourth row is the mean of September, October, November (SON), and the last row is the annual mean. Only areas where changes are significant at the 99% confidence level are shown. This figure is available in colour online at wileyonlinelibrary.com/journal/joc

additional warming due to natural vegetation dynamics: dynamic vegetation reduces the LULCC-driven cooling over land to 0.10 °C (FiNa *vs* DyLUC). This is due to the natural vegetation's response to climate change (e.g. northward shift of vegetation) and the resultant albedo changes. Without LULCC, natural vegetation dynamics cause a global warming over land of about 0.13 °C (Figure 3(a), DyNa *vs* FiNa), amplifying the radiative forcing of increased GHG-concentrations. This amplification is stronger than that with LULCC (DyLUC *vs* FiLUC, 0.11 °C) because the GHG forcing is not partially compensated by an LULCC-driven cooling and because the natural vegetation's dynamics are not partially overridden by land-use change.

Precipitation change over land (Figure 3(b)) had followed the same pattern as temperature change until 1980, but then temperatures increased rapidly, while precipitation did not. From 1980 onwards, the strongest increase in temperatures and precipitation *in relative terms* is in the boreal zone, but while this temperature increase is clearly reflected in the global average temperature over land, the precipitation increase cannot be recognized as clearly at

this scale. This is because the total global precipitation is strongly dominated by the much higher tropical rainfall, which is affected less by climate change as simulated by SPEEDY.

3.3. Effects of LULCC

Regionally, the effects of LULCC (Figure 4, first column, experiment FiLUC minus FiNa and DyLUC minus FiNa) are much stronger than those at the global level. Particularly in the mid latitudes, where the extent of deforestation (Figure 4(a) and (c)), albedo increase (Figure 4(d) and (f)), and reduced evapotranspiration (Figure S2(o) in Supporting Information 3 and Figure 5(o)) is most pronounced, LULCC causes a regional cooling of up to 1.5 °C, and the area of statistically significant ($p = 0.01$) cooling also spreads to outside the area than where LULCC actually occurs (Figure 4(g) and (i)).

The strongest cooling is simulated for western Russia and eastern China and is most pronounced in Northern Hemispheric winter (December, January, February; DJF) and spring (March, April, May; MAM) (Figures 5(a) and (d) and S2(a) and (d), Supporting Information 3), because

then the higher albedo of deforested land is amplified by snow. There is a positive feedback here because the cooling causes snow to melt later in spring, increasing the albedo for a longer period.

In tropical areas of Africa, South America and India, the cooling effect of LULCC is less pronounced because the higher albedo (and thus reduced SSR) is counter-balanced by reduced evapotranspiration (LHF), as described in Figure 1 for the (sub)tropics. The reduced evapotranspiration, both annually and seasonally (Figure S2, third column, in Supporting Information 3 and also Figure 5, third column), also reduces convective cloud formation and convective precipitation (especially in Africa, see Figure 4(j)), lowering evapotranspiration and thus forming a positive feedback loop. Reduced cloud cover decreases albedo. Therefore, the initial increase of surface albedo is counter-balanced by reduced cloud formation and thus a reduced decrease in SSR (Figure S2, Supporting Information 3, second column, and also Figure 5, second column).

In North America and Australia, there is little significant cooling where land-use and land-cover has changed (Figure 4(g)), even though there is a significant reduction in SSR, which is stronger than the reduction in LHF (see Figure 5(n) and (o) and Figure S2(n) and (o), Supporting Information 3).

3.4.   Effects of natural vegetation dynamics

The second column in Figure 4 (i.e. experiment DyNa minus FiNa) shows that vegetation patterns shift due to climate change and also due to CO_2 fertilization. In particular, there is a significant increase in tree cover in several regions of the world. The strongest increase is located in the northern high latitudes, especially in northeast Siberia where trees spread into the boreal tundra (Figure 4(b)). This is less pronounced in Alaska and Canada, as there is already an initial overestimation of tree cover (Figure 2(a)). The corresponding decrease in albedo causes a regional yearly average warming of up to 0.7 °C (Figure 4(e) and (h)) and even more at the seasonal level, especially in JJA (June, July, August; see Figure S3(g), Supporting Information 3 and also Figure 5(g)). In other areas, there is limited change, except for southern Africa, where a greening of the arid regions can be observed (Figure 4(b)) due to an increase in precipitation (Figure 4(k)) combined with an increased water-use efficiency due to higher atmospheric CO_2 concentrations. No significant remote effects can be identified: changes in climatology are restricted to the areas with changing vegetation cover (mainly increases of tree cover).

3.5.   Combined effects of LULCC and dynamic vegetation

The last column of Figure 4 (experiment DyLUC minus FiNa) shows the *combined* effects of both LULCC and dynamic vegetation. The changes due to LULCC alone (first column) dominate; the climatic response in those

regions where changes in natural vegetation are overruled by LULCC also dominate at the seasonal level (Figure 5) (e.g. central Asia and United States). Because LULCC masks several regions that would become greener due to natural vegetation's dynamics, the area of actual greening (i.e. increased tree cover) is mainly restricted to north-east Siberia and, to a lesser extent, west Canada and Alaska. Only in Siberia, a significant warming can be observed as a direct consequence of the relative large albedo decrease (Figure 4(f)) and thus SSR increase (Figure 5, second column), which overrules the corresponding increase in LHF (third column). Also, the boreal greening prevents the LULCC-driven cooling in west Russia from spreading northwards as observed in case of LULCC only (see Section 3.2, Figures 4(i) and 5, first column).

At higher latitudes, the decrease in SSR due to increased albedo after deforestation is only partly counter-balanced by a reduced energy flux to the atmosphere via latent heat (evapotranspiration; Figure 5). In the Tropics, the same mechanisms apply, but the feedback via cloud formation is stronger; surface albedo is similarly increased after deforestation, but cloud albedo is reduced due to reduced evapotranspiration and cloud formation. Therefore, the LULCC-driven cooling is less pronounced in the Tropics. As precipitation seasonality in the Tropics is not as uniform as temperature seasonality in the higher latitudes, the compensation of changes in SSR and LHF cannot be attributed to specific 3-month intervals.

4.   Discussion and conclusions

We have demonstrated that global forest cover, its temporal dynamics, and its effect on climate can be simulated well in our coupled DGVM–AGCM model. Our results specifically show that historic LULCC and shifting natural vegetation patterns not only had strong impacts on regional climate but also significantly affected the global average climate over land. Similarly, an earlier LPJ-based study showed that past LULCC affected river discharge at the global level (Gerten *et al.*, 2008), providing additional evidence for the global biogeophysical impact of human land-use changes.

Matthews *et al.* (2004) conducted one of the few studies that explicitly deals with both LULCC and dynamic natural vegetation. As in our study, Matthews *et al.* (2004) found that historic LULCC caused a significant cooling and both studies find that natural vegetation's dynamics act as a positive feedback on temperatures. If radiative forcing causes a warming, it is amplified by natural vegetation's dynamics. If LULCC reduces this warming, natural vegetation's response to this reduced warming is also smaller (i.e. the amplification of the dampened warming is smaller).

Even though there is no general disagreement between Matthews *et al.* (2004) and our study, the impact strengths differ considerably. Matthews *et al.* (2004) find that there is only little impact of LULCC on ocean temperatures; hence, we can assume that prescribing SSTs in

our study does not bias results significantly. The cooling impact of LULCC in our study is 0.20 to 0.22 °C over land (see Section 3.2), accounting for total agricultural land (cropland + pastures). Assuming that there is no oceanic temperature response (Matthews *et al.*, 2004), we find a global cooling of about 0.06 °C, while Matthews *et al.* (2004) find a global cooling of 0.13 °C since 1700 if only cropland expansion, and no other climate forcings, are being considered. Thus, our simulated impact of LULCC on global temperatures is smaller than that simulated by Matthews *et al.* (2004), even though we account for total LULCC and not only cropland since 1700. Causes of this difference may be the more detailed representation of cropland in our study (simulated as grassland in Matthews *et al.* (2004)) as well as the initial patterns of natural vegetation. Patterns of natural vegetation, which are computed internally in both models (LPJmL or Top-down Representation of Interactive Foliage and Flora Including Dynamics TRIFFID), may differ considerably, also reflecting the differences in climate patterns. One example in our case is the warm and dry bias in Central North America, where SPEEDY–LPJmL underestimates tree cover. Conversions from natural vegetation to cropland/rangeland in this region are therefore of reduced impact in our model.

Our simulations principally demonstrate that historic deforestation has caused local and regional cooling, especially in Eurasia and China. In the Tropics, the cooling was less pronounced due to reduced evapotranspiration, cloud formation, and precipitation. The recent boreal greening (Lucht *et al.*, 2002) had a significant warming effect in our simulations, especially in north-east Siberia, which has also been confirmed by other studies that consider albedo changes as the dominant factor in the boreal regions. (Govindasamy *et al.*, 2001; Bounoua *et al.*, 2002; Matthews *et al.*, 2004; Brovkin *et al.*, 2006; Bala *et al.*, 2007).

An inevitable disadvantage of dynamically coupling DGVMs with GCMs is that distortions in climate simulations directly affect the vegetation distribution, which sometimes amplifies the climate distortion: for example, SPEEDY–LPJmL overestimates precipitation on the southern Arabian Peninsula (Figure 2(c)), also with prescribed, observed vegetation patterns (not shown). This overestimation becomes even stronger if vegetation patterns are not prescribed and trees can establish due to the initial overestimation of precipitation. Implementing dynamic vegetation therefore means introducing another source of uncertainty to climate simulations, e.g. simulating ocean dynamics instead of prescribing SSTs. On the other hand, as shown by this study, anthropogenic LULCC and natural vegetation dynamics are important drivers of global and especially regional climate change and need to be jointly accounted for in climate simulations.

Globally, and also in most regions, LULCC proved to be far more important than dynamic vegetation in terms of its impact on climate. This, however, was only shown for the historic past here, when the magnitude of climate change was small, while land-use patterns have been changing strongly. As both future climate change (Scholze *et al.*, 2006) and future land-use change (Müller *et al.*, 2007; Lotze-Campen *et al.*, 2008) yield the potential to strongly affect global vegetation patterns, vegetation dynamics and LULCC may both become as important as LULCC was in the past.

The next generation of future climate simulations should therefore critically evaluate the pros and cons of implementing dynamic vegetation in climate models. As changes in albedo and the hydrological cycle are the dominant drivers through which vegetation dynamics affect climate, more attention should be paid to the parameterization of albedo and soil water–vegetation interaction. Here, we use simple global assumptions for albedo, while, for example, a finer distinction of different soil and vegetation types would be possible. Also, we did not consider irrigation in this study, which affects the partitioning between evapotranspiration and runoff (Rost *et al.*, 2008) and could affect local and regional climate considerably, especially in semi-arid regions with large irrigated agricultural areas as in the United States, China, and India (Boucher *et al.*, 2004; Betts *et al.*, 2007; Pielke *et al.*, 2007).

Climate mitigation policies do not generally consider the effects of LULCCs on the climate system (Marland *et al.*, 2003). However, large-scale biofuel production or afforestation could, as indicated above, have a variety of unanticipated impacts on global and regional climate (Pielke *et al.*, 2002; Schaeffer *et al.*, 2006) that go beyond the radiative forcing of the regulated GHGs. Therefore, a more complete indication of human contributions to climate change will require the climatic influences of land surface conditions and other processes to be considered in climate change mitigation strategies.

References

Avissar R, Werth D. 2005. Global hydroclimatological teleconnections resulting from tropical deforestation. *Journal of Hydrometeorology* **6**: 134–145.

Bala G, Caldeira K, Wickett M, Phillips TJ, Lobell DB, Delire C, Mirin A. 2007. Combined climate and carbon-cycle effects of large-scale deforestation. *Proceedings of the National Academy of Sciences of the United States of America* **104**: 6550–6555, DOI: 6510.1073/pnas.0608998104.

Betts RA. 2001. Biogeophysical impacts of land use on present-day climate: near-surface temperature change and radiative forcing. *Atmospheric Science Letters* **2**: 39–51, DOI: 10.1006/asle.2001.0037.

Betts RA, Boucher O, Collins M, Cox PM, Falloon PD, Gedney N, Hemming DL, Huntingford C, Jones CD, Sexton DMH, Webb MJ. 2007. Projected increase in continental runoff due to plant responses to increasing carbon dioxide. *Nature* **448**: U1037–U1035, DOI: 1010.1038/nature06045.

Bonan GB, Levis S. 2006. Evaluating aspects of the community land and atmosphere models (CLM3 and CAM3) using a Dynamic Global Vegetation Model. *Journal of Climate* **19**: 2290–2301.

Bondeau A, Smith P, Zaehle S, Schaphoff S, Lucht W, Cramer W, Gerten D, Lotze-Campen H, Müller C, Reichstein M, Smith B. 2007. Modelling the role of agriculture for the 20th century global terrestrial carbon balance. *Global Change Biology* **13**: 679–706, DOI: 10.1111/j.1365–2486.2006.01305.x.

Boucher O, Myhre G, Myhre A. 2004. Direct human influence of irrigation on atmospheric water vapour and climate. *Climate Dynamics* **22**: 597–603, DOI: 10.1007/s00382-00004-00402-00384.

Bounoua L, DeFries R, Collatz GJ, Sellers P, Khan H. 2002. Effects of land cover conversion on surface climate. *Climatic Change* **52**: 29–64.

Bracco A, Kucharski F, Molteni F, Hazeleger W, Severijns C. 2007. A recipe for simulating the interannual variability of the Asian summer monsoon and its relation with ENSO. *Climate Dynamics* **28**: 441–460, DOI: 10.1007/s00382-00006-00190-00380.

Brovkin V, Claussen M, Driesschaert E, Fichefet T, Kicklighter D, Loutre M, Matthews H, Ramankutty N, Schaeffer M, Sokolov A. 2006. Biogeophysical effects of historical land cover changes simulated by six Earth system models of intermediate complexity. *Climate Dynamics* **26**: 1–14, DOI: 10.1007/s00382-00005-00092-00386.

Brovkin V, Levis S, Loutre MF, Crucifix M, Claussen M, Ganopolski A, Kubatzki C, Petoukhov V. 2003. Stability analysis of the climate-vegetation system in the northern high latitudes. *Climatic Change* **57**: 119–138.

Chase TN, Pielke RA, Kittel TGF, Nemani RR, Running SW. 2000. Simulated impacts of historical land cover changes on global climate in northern winter. *Climate Dynamics* **16**: 93–105.

Claussen M. 1997. Modeling bio-geophysical feedback in the African and Indian monsoon region. *Climate Dynamics* **13**: 247–257.

Collatz G, Ribas-Carbo M, Berry J. 1992. Coupled photosynthesis-stomatal conductance model for leaves of C4 plants. *Australian Journal of Plant Physiology* **19**: 519–538.

Collatz GJ, Ball JT, Grivet C, Berry JA. 1991. Physiological and environmental-regulation of stomatal conductance, photosynthesis and transpiration – a model that includes a laminar boundary-layer. *Agricultural and Forest Meteorology* **54**: 107–136.

Cook BI, Bonan GB, Levis S, Epstein HE. 2008. Rapid vegetation responses and feedbacks amplify climate model response to snow cover changes. *Climate Dynamics* **30**: 391–406, DOI: 10.1007/s00382-00007-00296-z.

Costa MH, Foley JA. 2000. Combined effects of deforestation and doubled atmospheric CO_2 concentrations on the climate of Amazonia. *Journal of Climate* **13**: 18–34.

Cowling SA, Shin Y, Pinto E, Jones CD. 2008. Water recycling by Amazonian vegetation: coupled versus uncoupled vegetation-climate interactions. *Philosophical Transactions of the Royal Society B-Biological Sciences* **363**: 1865–1871, DOI: 10.1098/rstb.2007.0035.

Cox PM, Betts RA, Collins M, Harris PP, Huntingford C, Jones CD. 2004. Amazonian forest dieback under climate-carbon cycle projections for the 21st century. *Theoretical and Applied Climatology* **78**: 137–156.

Cox PM, Betts RA, Jones CD, Spall SA, Totterdell IJ. 2000. Acceleration of global warming due to carbon-cycle feedbacks in a coupled climate model. *Nature* **408**: 184–187.

Delire C, Foley JA, Thompson S. 2004. Long-term variability in a coupled atmosphere-biosphere model. *Journal of Climate* **17**: 3947–3959.

Dickinson RE, Oleson KW, Bonan G, Hoffman F, Thornton P, Vertenstein M, Yang ZL, Zeng XB. 2006. The Community Land Model and its climate statistics as a component of the Community Climate System Model. *Journal of Climate* **19**: 2302–2324.

Doherty R, Kutzbach J, Foley J, Pollard D. 2000. Fully coupled climate/dynamical vegetation model simulations over Northern Africa during the mid-Holocene. *Climate Dynamics* **16**: 561–573.

Farquhar GD, von Caemmerer S, Berry JA. 1980. A biochemical model of Photosynthetic CO_2 Assimilation in leaves of C3 Species. *Planta* **149**: 78–90.

Feddema JJ, Oleson KW, Bonan GB, Mearns LO, Buja LE, Meehl GA, Washington WM. 2005. The importance of land-cover change in simulating future climates. *Science* **310**: 1674–1678.

Findell KL, Shevliakova E, Milly PCD, Stouffer RJ. 2007. Modeled impact of anthropogenic land cover change on climate. *Journal of Climate* **20**: 3621–3634, DOI: 10.1175/jcli4185.3621.

Foley JA, Levis S, Prentice IC, Pollard D, Thompson SL. 1998. Coupling dynamic models of climate and vegetation. *Global Change Biology* **4**: 561–579.

Friedlingstein P, Cox P, Betts RA, Bopp L, von Bloh W, Brovkin V, Cadule P, Doney S, Eby M, Fung I, Bala G, John J, Jones CD, Joos F, Kato T, Kawamiya M, Knorr W, Lindsay K, Matthews HD, Raddatz T, Rayner P, Reick C, Roeckner E, Schnitzler K-G, Schnur R, Strassmann K, Weaver AJ, Yoshikawa C, Zeng N. 2006. Climate-carbon cycle feedback analysis, results from the C^{4}MIP model intercomparison. *Journal of Climate* **19**: 3337–3353.

Gallimore R, Jacob R, Kutzbach J. 2005. Coupled atmosphere-ocean-vegetation simulations for modern and mid-Holocene climates: role of extratropical vegetation cover feedbacks. *Climate Dynamics* **25**: 755–776.

Gedney N, Valdes PJ. 2000. The effect of Amazonian deforestation on the northern hemisphere circulation and climate. *Geophysical Research Letters* **27**: 3053–3056.

Gerten D, Schaphoff S, Haberlandt U, Lucht W, Sitch S. 2004. Terrestrial vegetation and water balance – hydrological evaluation of a dynamic global vegetation model. *Journal of Hydrology* **286**: 249–270.

Gerten D, Rost S, von Bloh W, Lucht W. 2008. Causes of change in 20th century global river discharge. *Geophysical Research Letters* **35**: L20405.

Gleckler PJ, Taylor KE, Doutriaux C. 2008. Performance metrics for climate models. *Journal of Geophysical Research: Atmospheres* **113**: D06104, DOI: 10.01029/02007jd008972.

Govindasamy B, Duffy PB, Caldeira K. 2001. Land use changes and Northern Hemisphere cooling. *Geophysical Research Letters* **28**: 291–294.

Haarsma RJ, Campos EJD, Molteni F. 2003. Atmospheric response to South Atlantic SST dipole. *Geophysical Research Letters* **30**: 1864, DOI: 10.1029/2003gl017829.

Haarsma RJ, Hazeleger W. 2007. Extratropical atmospheric response to equatorial Atlantic cold tongue anomalies. *Journal of Climate* **20**: 2076–2091, DOI: 10.1175/jcli4130.2071.

Haarsma RJ, Selten FM, Opsteegh JD, Lenderink G, Liu Q. 1998. *ECBILT A Coupled Atmosphere Ocean Sea-Ice Model for Climate Predictability Studies*, KNMI: De Bilt, NL.

Hagen-Zanker A, Engelen G, Hurkens J, Vanhout R, Uljee I. 2006. *Map Comparison Kit 3: User Manual*. Research Institute for Knowledge Systems: Maastricht.

Hagen-Zanker A, Straatman B, Uljee I. 2005. Further developments of a fuzzy set map comparison approach. *International Journal of Geographical Information Science* **19**: 769–785, DOI: 10.1080/13658810500072137.

Hagen A. 2003. Fuzzy set approach to assessing similarity of categorical maps. *International Journal of Geographical Information Science* **17**: 235–249, DOI: 10.1080/13658810210157822.

Hazeleger W, Molteni F, Severijns C, Haarsma R, Bracco A, Kucharski F. 2003. SPEEDO: a flexible coupled model for climate studies. *Clivar Exchanges* **28**: 27–30.

van den Hurk BJJM, Viterbo P, Beljaars ACM, Betts AK. ECMWF. 2000. Offline validation of the ERA40 surface scheme, 43 pp.

Jahn A, Claussen M, Ganopolski A, Brovkin V. 2005. Quantifying the effect of vegetation dynamics on the climate of the last glacial maximum. *Climate of the Past* **1**: 1–7.

Jones PD, New M, Parker DE, Martin S, Rigor IG. 1999. Surface air temperature and its variations over the last 150 years. *Reviews of Geophysics* **37**: 173–199.

Kleidon A, Fraedrich K, Heimann M. 2000. A green planet versus a desert world: estimating the maximum effect of vegetation on the land surface climate. *Climatic Change* **44**: 471–493.

Klein Goldewijk K, Bouwman AF, Drecht Gv. 2007. Mapping contemporary global cropland and grassland distributions on a 5 by 5 minute resolution. *Journal of Land Use Science* **2**: 167–190.

Koster RD, Guo ZC, Dirmeyer PA, Bonan G, Chan E, Cox P, Davies H, Gordon CT, Kanae S, Kowalczyk E, Lawrence D, Liu P, Lu CH, Malyshev S, McAvaney B, Mitchell K, Mocko D, Oki T, Oleson KW, Pitman A, Sud YC, Taylor CM, Verseghy D, Vasic R, Xue YK, Yamada T. 2006. GLACE: the global land-atmosphere coupling experiment. Part I: Overview. *Journal of Hydrometeorology* **7**: 590–610.

Kucharski F, Bracco A, Yoo JH, Molteni F. 2007. Low-frequency variability of the Indian monsoon-ENSO relationship and the tropical atlantic: the "Weakening" of the 1980s and 1990s. *Journal of Climate* **20**: 4255–4266, DOI: 10.1175/jcli4254.4251.

Kucharski F, Bracco A, Yoo JH, Molteni F. 2008. Atlantic forced component of the Indian monsoon interannual variability. *Geophysical Research Letters* **35**: L04706, DOI: 04710.01029/02007gl033037.

Kucharski F, Bracco A, Yoo JH, Tompkins AM, Feudale L, Ruti P, Dell'Aquila A. 2009. A Gill-Matsuno-type mechanism explains the tropical Atlantic influence on African and Indian monsoon rainfall. *Quarterly Journal of the Royal Meteorological Society* **135**: 569–579, DOI:10.1002/qj.1406.

Levis S, Bonan GB. 2004. Simulating springtime temperature patterns in the community atmosphere model coupled to the community land model using prognostic leaf area. *Journal of Climate* **17**: 4531–4540.

Lotze-Campen H, Müller C, Bondeau A, Rost S, Popp A, Lucht W. 2008. Global food demand, productivity growth and the scarcity of land and water resources: a spatially explicit mathematical programming approach. *Agricultural Economics* **39**: 325–338, DOI: 10.1111/j.1574-0862.2008.00336.x.

Loveland TR, Reed BC, Brown JF, Ohlen DO, Zhu Z, Yang L, Merchant JW. 2000. Development of a global land cover characteristics database and IGBP DISCover from 1 km AVHRR data. *International Journal of Remote Sensing* **21**: 1303–1330.

Lucht W, Prentice IC, Myneni RB, Sitch S, Friedlingstein P, Cramer W, Bousquet P, Buermann W, Smith B. 2002. Climatic control of the high-latitude vegetation greening trend and pinatubo effect. *Science* **296**: 1687–1689.

Mabuchi K, Sato Y, Kida H. 2005. Climatic impact of vegetation change in the Asian tropical region. Part II: Case of the northern hemisphere winter and impact on the extratropical circulation. *Journal of Climate* **18**: 429–446.

Marland G, Pielke R, Apps M, Avissar R, Betts R, Davis K, Frumhoff P, Jackson S, Joyce L, Kauppi P, Katzenberger J, MacDicken K, Neilson R, Niles J, Niyogi D, Norby R, Pena N, Sampson N, Xue Y. 2003. The climatic impacts of land surface change and carbon management, and the implications for climate-change mitigation policy. *Climate Policy* **3**: 149–157.

Matthews HD, Weaver AJ, Eby M, Meissner KJ. 2003. Radiative forcing of climate by historical land cover change. *Geophysical Research Letters* **30**: 1055, DOI: 10.1029/2002gl016098.

Matthews HD, Weaver AJ, Meissner KJ, Gillett NP, Eby M. 2004. Natural and anthropogenic climate change: incorporating historical land cover change, vegetation dynamics and the global carbon cycle. *Climate Dynamics* **22**: 461–479, DOI:10.1007/s00382-00004-00392-00382.

Maynard K, Royer J-F. 2004a. Effects of "realistic" land-cover change on a greenhouse-warmed African climate. *Climate Dynamics* **22**: 343–358, DOI: 310.1007/s00382-00003-00371-z.

Maynard K, Royer JF. 2004b. Sensitivity of a general circulation model to land surface parameters in African tropical deforestation experiments. *Climate Dynamics* **22**: 555–572, DOI: 10.1007/s00382-00004-00398-00389.

Molteni F. 2003. Atmospheric simulations using a GCM with simplified physical parametrizations. I: model climatology and variability in multi-decadal experiments. *Climate Dynamics* **20**: 175–191.

Müller C, Eickhout B, Zaehle S, Bondeau A, Cramer W, Lucht W. 2007. Effects of changes in CO2, climate, and land use on the carbon balance of the land biosphere during the 21st century. *Journal of Geophysical Reseach: Biogeosciences* **112**: G02032, DOI: 10.01029/02006JG000388.

Müller C, Lucht W. 2007. Robustness of terrestrial carbon and water cycle simulations against variations in spatial resolution. *Journal of Geophysical Research: Atmospheres* **112**: D06105, DOI: 10.01029/02006JD007875.

Myhre G, Myhre A. 2003. Uncertainties in radiative forcing due to surface albedo changes caused by land-use changes. *Journal of Climate* **16**: 1511–1524.

Notaro M, Liu ZY. 2007. Potential impact of the Eurasian boreal forest on North Pacific climate variability. *Journal of Climate* **20**: 981–992, DOI: 10.1175/jcli4052.1171.

Notaro M, Liu ZY. 2008. Statistical and dynamical assessment of vegetation feedbacks on climate over the boreal forest. *Climate Dynamics* **31**: 691–712, DOI: 10.1007/s00382-00008-00368-00388.

Notaro M, Liu ZY, Gallimore R, Vavrus SJ, Kutzbach JE, Prentice IC, Jacob RL. 2005. Simulated and observed preindustrial to modern vegetation and climate changes. *Journal of Climate* **18**: 3650–3671.

O'Ishi R, Abe-Ouchi A, Prentice IC, Sitch S. 2009. Vegetation dynamics and plant CO2 responses as positive feedbacks in a greenhouse world. *Geophysical Research Letters* **36**: L11706, DOI: 10.11029/12009gl038217.

Opsteegh JD, Haarsma RJ, Selten FM, Kattenberg A. 1998. ECBILT: a dynamic alternative to mixed boundary conditions in ocean models. *Tellus A* **50**: 348–367.

Oyama MD, Nobre CA. 2004. Climatic consequences of a large-scale desertification in northeast Brazil: a GCM simulation study. *Journal of Climate* **17**: 3203–3213.

Pielke R, Marland G, Betts R, Chase T, Eastman J, Niles J, Niyogi D, Running S. 2002. The influence of land-use change and landscape dynamics on the climate system: relevance to climate-change policy beyond the radiative effect of greenhouse gases. *Philosophical Transactions of the Royal Society of London Series A-Mathematical Physical and Engineering Sciences* **360**: 1705–1719.

Pielke RA, Adegoke JO, Chase TN, Marshall CH, Matsui T, Niyogi D. 2007. A new paradigm for assessing the role of agriculture in the climate system and in climate change. *Agricultural and Forest Meteorology* **142**: 234–254, DOI: 10.1016/j.agrformet.2006.1006.1012.

Pitman A, de Noublet-Ducoudré N, Cruz FT, Davin EL, Bonan GB, Brovkin V, Claussen M, Delire C, Ganzeveld L, Gayler V, van den Hurk BJJM, Lawrence PJ, van der Molen MK, Müller C, Reick CH, Seneviratne SI, Strengers BJ, Voldoire A. 2009. Uncertainties in climate responses to past land cover change: First results from the LUCID intercomparison study. *Geophysical Research Letters* **36**: L14814, DOI: 10.11029/12009GL039076.

Ronda RJ, Haarsma RJ, Holtslag AAM. 2003. Representing the atmospheric boundary layer in climate models of intermediate complexity. *Climate Dynamics* **21**: 327–335.

Rost S, Gerten D, Heyder U. 2008. Human alterations of the terrestrial water cycle through land management. *Advances in Geosciences* **18**: 43–50.

Schaeffer M, Eickhout B, Hoogwijk M, Strengers B, van Vuuren D, Leemans R, Opsteegh T. 2006. CO2 and albedo climate impacts of extratropical carbon and biomass plantations. *Global Biogeochemical Cycles* **20**: Gb2020, DOI: 10.1029/2005 gb002581.

Scholze M, Knorr W, Arnell NW, Prentice IC. 2006. A climate-change risk analysis for world ecosystems. *Proceedings of the National Academy of Sciences* **103**: 13116–13120.

Sitch S, Smith B, Prentice I, Arneth A, Bondeau A, Cramer W, Kaplan J, Levis S, Lucht W, Sykes M, Thonicke K, Venevsky S. 2003. Evaluation of ecosystem dynamics, plant geography and terrestrial carbon cycling in the LPJ dynamic global vegetation model. *Global Change Biology* **9**: 161–185.

Solomon S, Qin D, Manning M, Chen Z, Marquis M, Averyt KB, Tignor M, Miller HL. 2007. *Climate Change 2007: The Physical Science Basis*. Contribution of Working Group I to the Fourth Assessment Report of the Intergovernmental Panel on Climate Change. Cambridge University Press: Cambridge, United Kingdom and New York.

Sterl A, van Oldenborgh GJ, Hazeleger W, Burgers G. 2007. On the robustness of ENSO teleconnections. *Climate Dynamics* **29**: 469–485, DOI: 10.1007/s00382-00007-00251-z.

Strengers B, Leemans R, Eickhout B, de Vries B, Bouwman L. 2004. The land-use projections and resulting emissions in the IPCC SRES scenarios as simulated by the IMAGE 2.2 model. *GeoJournal* **61**: 381–393.

Voldoire A, Royer JF. 2004. Tropical deforestation and climate variability. *Climate Dynamics* **22**: 857–874, DOI: 10.1007/s00382-00004-00423-z.

Xie P, Arkin PA. 1997. Global Precipitation: A 17-Year Monthly Analysis Based on Gauge Observations, Satellite Estimates, and Numerical Model Outputs. *Bulletin of the American Meteorological Society* **78**: 2539–2558.

Zhao M, Pitman AJ. 2002. The regional scale impact of land cover change simulated with a climate model. *International Journal of Climatology* **22**: 271–290.